Three-Site Mechanism and Molecular Weight: Time Dependency in Liquid Propylene Batch Polymerization Using a $MgCl_2$-Supported Ziegler-Natta Catalyst

FUMIHIKO SHIMIZU,[1] JOCHEM T. M. PATER,[2] GÜNTER WEICKERT[2]

[1] Mitsubishi Chemical Corporation, Yokohama Research Center, 1000, Kamoshida-cho, Aoba-ku, Yokohama, 227-8502, Japan

[2] Process Technology Institute Twente, University of Twente, P.O. Box 217, 7500 AE Enschede, The Netherlands

Received 22 November 1999; accepted 3 November 2000

ABSTRACT: This article demonstrates that the molecular weight of propylene homopolymer decreases with time, and that the molecular weight distribution (MWD) narrows when a highly active $MgCl_2$-supported catalyst is used in a liquid pool polymerization at constant H_2 concentration and temperature. To track the change in molecular weight and its distribution during polymerization, small portions of homo polymer samples were taken during the reaction. These samples were analyzed by Cross Fractionation Chromatograph (CFC), and the resulting data were treated with a three-site model. These analyses clearly showed that the high molecular weight fraction of the distribution decreases as a function of time. At the same time, the MWD narrows because the weight-average molecular weight decreases faster than the number-average molecular weight. A probable mechanism based on the reaction of an external donor with $AlEt_3$ is proposed to explain these phenomena. © 2001 John Wiley & Sons, Inc. J Appl Polym Sci 81: 1035–1047, 2001

Key words: $MgCl_2$-supported Ziegler-Natta catalyst; liquid pool propylene polymerization; molecular weight; time dependency; three-site model

INTRODUCTION

The behavior of highly active $MgCl_2$-supported Ziegler-Natta catalysts has been widely investigated due to their commercial importance.[1] Previous kinetics studies have been extensively reviewed by Albizatti et al.[1] However, despite the industrial importance of the liquid pool polymerization process, there is a lack of data with respect to at least two important topics related to this process: (a) the time dependency of the molecular weight produced, and (b) data on catalyst performance in liquid phase propylene polymerization. Another problem in describing the commercial process is the relationship between the kinetics and the residence time distribution (RTD) of the catalyst contained in polymer particles in the continuous reactors used in industrial PP production. However, if the RTD is known, it is relatively easy to couple batch kinetics with a model of the RTD of a given reactor to compute particle size distribution, activity distribution, and finally thermal reactor behavior, see, for example, Prasetya et al.[2]

To resolve these problems, Tanaka et al.[3] began by investigating the influence of time on various catalyst performances in liquid pool propylene polymerization with a highly active $MgCl_2$-supported Ziegler-Natta catalyst. At the same time, a calorimetric method for measuring

Correspondence to: F. Shimizu.

Journal of Applied Polymer Science, Vol. 81, 1035–1047 (2001)

the polymerization rate in liquid propylene polymerization was developed at the Twente University, see Samson et al.[4,5] In the current work, we improved upon the method used by Samson[4,5] by installing an on-line sampling system, which allows us to measure the evolution of polymer properties as a function of time. This new technique led to the observation that the molecular weight of polypropylene (PP) produced on a growing polymer particle decreases with time, and that the MWD of PP narrows with time, even at constant temperature and constant hydrogen concentration. The objectives of this article are to describe the phenomenon in detail and to clarify the mechanism.

EXPERIMENTAL

Polymerization Procedure

The details of the setup are as described by Samson et al.[4] with the exception that the reactor was equipped with a sampling system. Polymerizations were carried out batchwise under isothermal conditions. During the polymerization, small amounts of PP samples were withdrawn at intervals of 30 min. It was found that withdrawing small amounts of samples has practically no influence on polymerization kinetics. The samples were analyzed by CFC to determine the average molecular weight and the MWD.

The catalyst used in the current work was a highly active supported catalyst of type $MgCl_2$/$TiCl_4$/DEP-TEA/ED, where DEP, TEA, and ED represent diethyl phthalate, triethyl aluminum, and external donor, respectively. As the ED, *t*-BuEtSi$(OMe)_2$ was used in this study. In a typical experiment, the 5-liter reactor described above was initially charged with different, known amounts of H_2 and 2600 mL of liquid propylene. The reactor was then heated, and when the rector temperature reached 70°C, 170 mg of TEA and the sufficient amount of ED to maintain a molar ratio of ED/TEA = 0.03 were added. Next, 4 mg of solid catalyst component was injected to start the polymerization. During the polymerization, a master–slave PID controller regulated the reactor temperature at 70°C with an accuracy of 0.1 K. Approximately 6 g of PP powder per sample was withdrawn during the polymerization. The polymerization was terminated after 2 h by rapidly flashing off the unreacted propylene.

Crossfractionation Chromatography (CFC)

PP samples withdrawn from the reactor were analyzed by crossfractionation chromatography (CFC T-102L, Mitsubishi Chemical Co., Japan) with *o*-dichlorobenzene as an extraction solvent. As an antioxidant, BHT was solved in *o*-dichlorobenzene (ca. 2 mg/mL). Approximately 1 mg of the PP sample was loaded onto a column containing glass beads at 135°C, and the column was cooled to 40°C at intervals of 3°C. In each step, the column temperature was held for 10 min. Then the column temperature was raised and stepwise elution was carried out at 40, 95, 100, 105, 109, 111, 113, 115, 117, 119, 121, 123, 125, and 135°C. Each fraction was analyzed by GPC attached to the CFC system.

RESULTS AND DISCUSSION

Kinetics

The kinetics of the Ziegler-Natta catalyst can generally be described with a first-order model with the assumption that (a) the rate of polymerization is directly proportional to monomer and active site concentrations, (b) the active site concentration decreases in accordance with first-order decay, and (c) there are no mass transport limitations in the growing polymer particles. These assumptions are usually approximately correct when we use a $MgCl_2$-supported catalyst where a combination of a diester and an alkoxysilane is used. Thus, we can write:

$$R_p = k_p C_m C^*$$

$$\frac{dC^*}{dt} = -k_d C^* \tag{1}$$

where R_p is the rate of polymerization, k_p is a constant, C_m and C^* are the monomer and the active site concentrations, and k_d is a decay constant. Note that C_m remains constant in liquid pool polymerizations under equilibrium conditions. From these two equations, the next equation, which describes the relationship between time and R_p, is obtained:

$$R_p = R_{p,o}\exp(-k_d t) \tag{2}$$

where $R_{p,o}$ is the initial R_p.

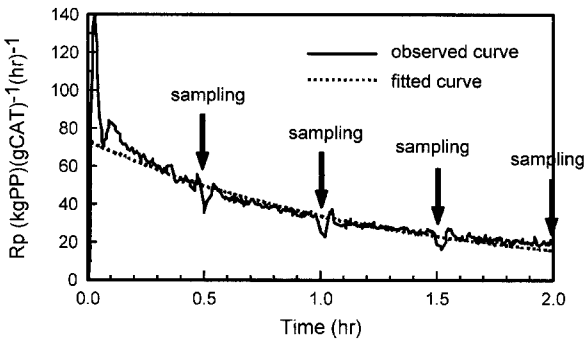

Figure 1 The kinetics of PP homo polymerization at 70°C with $[H_2]$ of 8.0 vol %.

Three runs with different H_2 concentrations were initially carried out at 70°C. Figure 1 shows an example of the typical kinetic behavior of the PP homopolymerization reactions observed during the course of the current work with a constant H_2 concentration of 8% (v/v in the gas phase). We determined $R_{p,o}$ and k_d by a nonlinear least-squares method to obtain $R_{p,o}$ of 73.7 (kg-PP)(g-CAT)$^{-1}$ (h)$^{-1}$ and k_d of 0.769 h^{-1}. One can see that most of the kinetic curve is well fitted by eq. (2), with the exception of the first few minutes of the reaction. The reason for this is that it is rather difficult to precisely control the temperature immediately after catalyst injection. Note that in such calorimetric measurements, small temperature deviations can lead to large apparent oscillations in R_p at the beginning of polymerization. In addition, it is clear that withdrawing small samples of PP powder during the reaction has practically no influence on the kinetics. We will discuss comprehensive kinetic studies later.

Molecular Weight—Time Dependency

Table I shows that weight-average molecular weight (M_w) decreases with reaction time. Number-average molecular weight (M_n) basically decreases as well, but the change is relatively small. Independently of our findings, Nakajima et al.[6] also found that melt flow rate (MFR) of PP increases with time when they use a $MgCl_2$-supported catalyst and alkoxysilanes as EDs. Because higher MFR means lower molecular weight, their results show that molecular weight of PP decreases with time. This is in accordance with our findings.

Table I Decrease in M_n and M_w with Time at 70°C[a]

Time (h)	$M_n \times 10^{-3}$			$M_w \times 10^{-3}$		
	Run 1	Run 2	Run 3	Run 1	Run 2	Run 3
0.5	72.2	49.4	41.3	402	269	221
1.0	64.6	47.3	41.8	385	246	211
1.5	68.2	47.7	39.0	376	244	199
2.0	66.7	46.3	39.9	360	234	199

[a] The H_2 concentration in the gas phase of the reactor in the run 1, 2, and 3 was 4.7, 8.0, and 11.0 vol %, respectively.

Table II The Result of H_2 Concentration Measurement at 70°C

Time (h)	0.5	1.0	1.5	2.0
$[H_2]$ (vol %)[a]	6.9	4.5	4.2	4.1

[a] H_2 concentration in the gas phase of the reactor.

One might think that a decrease in molecular weight is caused by increase in H_2 concentration in the reactor. However, this is quite unlikely because: (a) H_2 was injected into the reactor only once before starting polymerization, see above; (b) it is well known that H_2 is not generated in propylene polymerizations with $MgCl_2$-supported Ziegler-Natta catalyst because β-H elimination is negligible.[1] In a separate experiment, gas chromatography (GC) was used to confirm the fact that H_2 concentration remained constant and does not increase with time. In fact, Table II shows that the H_2 concentration slightly decreases with time. This means that H_2 is consumed during polymerization, as proposed by Spitz et al.[7] This allows us to conclude that the decrease in molecular weight during polymerization is not caused by increase in H_2 concentration; rather, another explanation must be found.

We also investigated the relationship between reaction time and molecular weight distribution (M_w/M_n). Table III shows that M_w/M_n basically decreases with time, i.e., molecular weight distribution narrows as the reaction progresses.

CFC Measurement

In the previous sections it was mentioned that both M_w and M_w/M_n decrease with reaction time. What kind of mechanism causes these phenomena? Is there a good way to draw conclusions on the polymerization mechanism?

If we were able to "observe" the active sites directly in some way, such as spectroscopic method, we might obtain information related to

Table III Decrease in M_w/M_n with Time at 70°C[a]

	M_w/M_n		
Time (h)	Run 1	Run 2	Run 3
0.5	5.57	5.45	5.35
1.0	5.95	5.21	5.04
1.5	5.51	5.12	5.10
2.0	5.40	5.05	4.99

[a] The H_2 concentration in the gas phase of the reactor in the run 1, 2, and 3 was 4.7, 8.0, and 11.0 vol %, respectively.

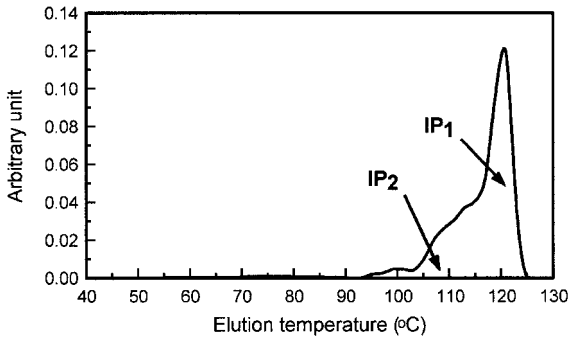

Figure 2 A typical TREF diagram of isotactic PP.

the mechanism of these phenomena. Unfortunately, it is impossible to observe the active sites directly because (a) the active sites concentration is quite low, (b) it is practically impossible to distinguish active Titanium ion from inactive ones, and (c) the active sites are unstable, especially in the working state. Therefore, we must look for another method to obtain useful information to find the mechanism.

In the long history of the research on Ziegler-Natta catalysts, the analysis of PP produced with the catalysts has played an important role.[8] Based on such analysis data, researchers have drawn many useful conclusions about the mechanism of Ziegler-Natta catalysts by reasonable speculation. In our case, CFC seems to work for our purpose. CFC is a powerful tool for analysis of PP. One can obtain information concerning molecular weight distribution and stereo-regularity distribution simultaneously. In this study, we added a factor of time by withdrawing PP samples at some intervals during polymerization. The combined information of molecular weight distribution, stereo-regularity distribution, and their reaction time dependency should help us to find the mechanism.

A typical CFC diagram of PP obtained with the catalyst system used in the current work is shown in Figure 2, and is explained below. We analyzed 12 PP samples shown in Table III by CFC. The results of the CFC measurements are shown in Tables IV–XV.

Three-Site Model

Before analyzing the CFC data, let us look for a moment at the concept of the heterogeneity of active sites in $MgCl_2$-supported Ziegler-Natta catalysts. Generally speaking, Ziegler-Natta catalysts for PP such as $TiCl_3$ catalysts or $MgCl_2$-supported catalysts produce isotactic PP (IP) and atactic PP (AP). With respect to isotactic PP, Kakugo et al.[9–11] proposed that it is classified into two types of homo PP: IP_1 and IP_2, where IP_1 is a highly isotactic part, and IP_2 is a less isotactic part. Figure 2 shows that isotactic PP is classified into IP_1 and IP_2 in our catalyst system as well. However, because it is not possible to take fractionation data below 40°C with our CFC equipment, the AP fraction cannot be seen in Figure 2. Note that the peak of AP is in the area lower than this temperature due to its low crystallinity. Nevertheless, it is clear that PP homopolymer can be classified into three parts, i.e. AP, IP_2, and IP_1.

Cheng[12] proposed that a three-site model comprised of two enantiomorphic sites and a chain-end-control site gives a good fit for the observed ^{13}C-NMR data in terms of microtacticity distribution. Kakugo[11] also proposed that AP, IP_1, and IP_2 are respectively produced on such three types of

Table IV The Results of CFC Measurement of the Sample 1-1 Withdrawn at 0.5 h in Run 1

Elution Temperature (°C)	Weight Fraction	M_n	M_w
40–95	0.046	8.876E+03	2.745E+04
95–100	0.004	1.171E+04	1.303E+04
100–105	0.024	2.240E+04	4.312E+04
105–109	0.047	4.565E+04	7.276E+04
109–111	0.022	4.896E+04	7.551E+04
111–113	0.029	5.574E+04	8.461E+04
113–115	0.035	6.505E+04	1.021E+05
115–117	0.054	6.776E+04	1.227E+05
117–119	0.086	1.058E+05	1.845E+05
119–121	0.245	1.532E+05	3.189E+05
121–123	0.311	2.259E+05	6.037E+05
123–125	0.099	4.671E+05	1.049E+06

Table V The Results of CFC Measurement of the Sample 1-2 Withdrawn at 1.0 h in Run 1

Elution Temperature (°C)	Weight Fraction	M_n	M_w
40–95	0.045	8.057E+03	2.556E+04
95–100	0.010	1.271E+04	2.034E+04
100–105	0.026	2.854E+04	5.947E+04
105–109	0.054	3.506E+04	6.511E+04
109–111	0.019	4.573E+04	6.527E+04
111–113	0.030	5.033E+04	8.007E+04
113–115	0.040	5.929E+04	9.939E+04
115–117	0.056	7.208E+04	1.296E+05
117–119	0.101	9.471E+04	1.876E+05
119–121	0.246	1.433E+05	3.226E+05
121–123	0.289	2.017E+05	6.091E+05
123–125	0.084	4.743E+05	1.071E+06

Table VII The Results of CFC Measurement of the Sample 1-4 Withdrawn at 2.0 h in Run 1

Elution Temperature (°C)	Weight Fraction	M_n	M_w
40–95	0.038	8.066E+03	1.871E+04
95–100	0.004	8.392E+03	1.001E+04
100–105	0.032	2.291E+04	4.961E+04
105–109	0.059	3.829E+04	6.696E+04
109–111	0.023	4.275E+04	6.635E+04
111–113	0.031	4.846E+04	7.613E+04
113–115	0.041	5.797E+04	9.457E+04
115–117	0.058	6.882E+04	1.199E+05
117–119	0.112	9.658E+04	1.819E+05
119–121	0.271	1.425E+05	3.337E+05
121–123	0.270	2.410E+05	6.240E+05
123–125	0.061	4.515E+05	9.709E+05

active sites as nonstereospecific sites, less isospecific sites, and highly isospecific sites.[13] Furthermore, Härkönen et al.[14] proposed that there are three types of active sites in $MgCl_2$-supported Ziegler-Natta catalysts: highly isospecific enantiomorphic sites, less isospecific enantiomorphic sites, and relatively syndiospecific sites obeying Bernoullian statistics. Corradini et al.[8] also proposed that the active sites on $MgCl_2$-supported catalyst are classified into isotactic site, isotactoid site, and syndiotactoid site. Because atactic PP is rich in syndiotactic sequences,[15,16] the conclusions of Härkönen et al. and Corradini et al. are basically the same as those proposed by Kakugo and his coworkers. Recently, Busico et al.[17] demonstrated more direct evidence for three-site model based on high-resolution ^{13}C-NMR data at heptad/nonad level. Thus, it is reasonable to classify the active sites on $MgCl_2$-supported Ziegler-Natta catalyst into three types. In the remainder of this work, we call these three types of active sites "type A," "type B," and "type C" for the simplicity, where the type A site produces atactic PP, the type B site produces less isotactic PP, and the type C site produces highly isotactic PP. Interestingly, each site has a different H_2 response, i.e., each active site produces PP with different molecular weight.[8,18,19] The type A site generally produces low molecular weight PP,

Table VI The Results of CFC Measurement of the Sample 1-3 Withdrawn at 1.5 h in Run 1

Elution Temperature (°C)	Weight Fraction	M_n	M_w
40–95	0.041	7.868E+03	2.179E+04
95–100	0.004	1.047E+04	1.222E+04
100–105	0.031	2.447E+04	5.619E+04
105–109	0.054	4.056E+04	7.055E+04
109–111	0.020	4.410E+04	6.475E+04
111–113	0.030	5.302E+04	8.493E+04
113–115	0.041	6.138E+04	1.008E+05
115–117	0.057	7.795E+04	1.358E+05
117–119	0.107	9.909E+04	1.890E+05
119–121	0.255	1.527E+05	3.344E+05
121–123	0.284	2.358E+05	6.146E+05
123–125	0.077	4.331E+05	9.636E+05

Table VIII The Results of CFC Measurement of the Sample 2-1 Withdrawn at 0.5 h in Run 2

Elution Temperature (°C)	Weight Fraction	M_n	M_w
40–95	0.050	6.446E+03	1.220E+04
95–100	0.006	8.026E+03	9.567E+03
100–105	0.035	2.107E+04	4.136E+04
105–109	0.071	3.326E+04	6.065E+04
109–111	0.029	3.890E+04	5.873E+04
111–113	0.040	4.477E+04	7.339E+04
113–115	0.049	5.396E+04	8.890E+04
115–117	0.070	6.384E+04	1.178E+05
117–119	0.116	8.657E+04	1.653E+05
119–121	0.246	1.293E+05	2.800E+05
121–123	0.244	1.913E+05	4.887E+05
123–125	0.045	4.400E+05	8.518E+05

Table IX The Results of CFC Measurement of the Sample 2-2 Withdrawn at 1.0 h in Run 2

Elution Temperature (°C)	Weight Fraction	M_n	M_w
40–95	0.053	6.529E+03	1.294E+04
95–100	0.010	9.955E+03	1.273E+04
100–105	0.036	2.105E+04	3.856E+04
105–109	0.072	3.393E+04	5.844E+04
109–111	0.029	4.005E+04	5.943E+04
111–113	0.039	4.814E+04	7.374E+04
113–115	0.050	5.182E+04	8.444E+04
115–117	0.072	6.596E+04	1.177E+05
117–119	0.124	8.678E+04	1.644E+05
119–121	0.255	1.217E+05	2.766E+05
121–123	0.227	1.922E+05	4.803E+05
123–125	0.034	3.788E+05	6.927E+05

Table XI The Results of CFC Measurement of the Sample 2-4 Withdrawn at 2.0 h in Run 2

Elution Temperature (°C)	Weight Fraction	M_n	M_w
40–95	0.059	7.196E+03	1.686E+04
95–100	0.010	1.062E+04	1.332E+04
100–105	0.041	2.155E+04	4.071E+04
105–109	0.081	3.476E+04	6.233E+04
109–111	0.033	4.040E+04	6.413E+04
111–113	0.040	5.102E+04	7.734E+04
113–115	0.056	4.905E+04	8.405E+04
115–117	0.074	6.575E+04	1.178E+05
117–119	0.135	9.283E+04	1.752E+05
119–121	0.257	1.205E+05	2.813E+05
121–123	0.194	2.059E+05	4.866E+05
123–125	0.022	4.739E+05	8.352E+05

while the type C site generally produces high molecular weight PP, and the type B site produces PP with medium molecular weight. Accordingly, we can characterize these three types of active sites, as shown in Table XVI (see also the footnote).[20]

We then analyzed the CFC data in accordance with the three-site model. We attributed the fraction eluted from 40 to 95°C to fraction A, the fraction eluted from 95 to 111°C to fraction B, and the fraction eluted from 111 to 125°C to fraction C. The weight ratio of the fraction A, B, and C is approximately 0.04–0.06/0.08–0.20/0.74–0.88 (see Figs. 5–7). This distribution well agrees with the data obtained by Härkönen et al.[14] Thus, we can say that our classification in terms of elution temperature is reasonable. Based on this classification, we calculated M_n and M_w for the fractions A, B, and C using a blending rule (3):

$$M_w = \sum_i w_i M_{w_i}$$

$$\frac{1}{M_n} = \sum_i \frac{w_i}{M_{n_i}} \tag{3}$$

where w_i, M_{w_i}, and M_{n_i} are weight fraction, weight-average molecular weight, and number-

Table X The Results of CFC Measurement of the Sample 2-3 Withdrawn at 1.5 h in Run 2

Elution Temperature (°C)	Weight Fraction	M_n	M_w
40–95	0.054	6.689E+03	1.303E+04
95–100	0.009	9.872E+03	1.197E+04
100–105	0.037	2.297E+04	3.957E+04
105–109	0.080	3.379E+04	5.916E+04
109–111	0.036	4.028E+04	6.549E+04
111–113	0.037	4.726E+04	6.959E+04
113–115	0.047	5.654E+04	8.521E+04
115–117	0.073	6.436E+04	1.130E+05
117–119	0.125	8.378E+04	1.600E+05
119–121	0.260	1.275E+05	2.818E+05
121–123	0.215	1.996E+05	4.924E+05
123–125	0.028	4.082E+05	7.291E+05

Table XII The Results of CFC Measurement of the Sample 3-1 Withdrawn at 0.5 h in Run 3

Elution Temperature (°C)	Weight Fraction	M_n	M_w
40–95	0.056	5.691E+03	1.087E+04
95–100	0.013	9.222E+03	1.279E+04
100–105	0.044	2.179E+04	4.545E+04
105–109	0.082	3.055E+04	5.659E+04
109–111	0.032	3.666E+04	5.805E+04
111–113	0.046	4.400E+04	7.283E+04
113–115	0.051	5.401E+04	8.622E+04
115–117	0.069	6.597E+04	1.100E+05
117–119	0.119	8.207E+04	1.567E+05
119–121	0.234	1.247E+05	2.687E+05
121–123	0.224	1.716E+05	4.268E+05
123–125	0.032	3.679E+05	6.408E+05

Table XIII The Results of CFC Measurement of the Sample 3-2 Withdrawn at 1.0 h in Run 3

Elution Temperature (°C)	Weight Fraction	M_n	M_w
40–95	0.051	5.230E+03	8.845E+03
95–100	0.012	8.054E+03	1.014E+04
100–105	0.048	2.357E+04	4.627E+04
105–109	0.076	3.686E+04	5.886E+04
109–111	0.037	4.174E+04	6.479E+04
111–113	0.049	4.804E+04	7.892E+04
113–115	0.056	5.250E+04	8.337E+04
115–117	0.075	6.525E+04	1.096E+05
117–119	0.141	8.326E+04	1.653E+05
119–121	0.242	1.186E+05	2.638E+05
121–123	0.189	1.936E+05	4.467E+05
123–125	0.023	3.856E+05	6.205E+05

Table XV The Results of CFC Measurement of the Sample 3-4 Withdrawn at 2.0 h in Run 3

Elution Temperature (°C)	Weight Fraction	M_n	M_w
40–95	0.066	6.653E+03	1.546E+04
95–100	0.010	1.100E+04	1.335E+04
100–105	0.048	2.258E+04	4.630E+04
105–109	0.098	2.997E+04	5.871E+04
109–111	0.035	3.602E+04	5.583E+04
111–113	0.050	4.090E+04	6.948E+04
113–115	0.059	4.889E+04	8.357E+04
115–117	0.087	6.067E+04	1.123E+05
117–119	0.134	8.861E+04	1.654E+05
119–121	0.239	1.250E+05	2.696E+05
121–123	0.161	2.202E+05	4.546E+05
123–125	0.014	4.696E+05	7.328E+05

average molecular weight of each component, respectively. Table XVII shows the summary of the calculation, where $w(A)$, $w(B)$, and $w(C)$ are the weight fraction of the PP produced from the type A, B, and C sites, respectively. $M_n(A)$, $M_n(B)$, and $M_n(C)$ are the number-average molecular weight of the PP produced on the type A, B, and C sites, respectively. Similarly, $M_w(A)$, $M_w(B)$, and $M_w(C)$ are the weight-average molecular weight produced from the type A, B, and C sites, respectively.

We then validated the blending rule that we used, and verified that the molecular weights of the real polymers[21] were reproduced in terms of M_n and M_w using the blending rule (3) based on the calculated values of $w(A)$, $w(B)$, $w(C)$, $M_n(A)$, $M_n(B)$, $M_n(C)$, $M_w(A)$, $M_w(B)$, and $M_w(C)$. The agreement of observed and calculated M_n and M_w for real polymers was very good (see Figs. 3 and 4). It can, therefore, be concluded that the blending rule of eq. (3) is valid for the calculation of M_n and M_w of the fraction A, B, and C.

Table XIV The Results of CFC Measurement of the Sample 3-3 Withdrawn at 1.5 h in Run 3

Elution Temperature (°C)	Weight Fraction	M_n	M_w
40–95	0.063	6.027E+03	1.216E+04
95–100	0.011	8.743E+03	1.107E+04
100–105	0.045	2.213E+04	4.088E+04
105–109	0.089	3.242E+04	5.689E+04
109–111	0.042	3.367E+04	5.840E+04
111–113	0.045	4.571E+04	7.001E+04
113–115	0.058	5.069E+04	8.266E+04
115–117	0.076	6.644E+04	1.097E+05
117–119	0.146	7.794E+04	1.643E+05
119–121	0.242	1.261E+05	2.644E+05
121–123	0.170	2.053E+05	4.409E+05
123–125	0.014	4.613E+05	6.951E+05

Mechanism of MW and MWD as a Function of Time

The evolution of $w(A)$, $w(B)$, and $w(C)$ as a function of time can be seen in Figures 5–7. First of all, it is clear that $w(A)$ does not change significantly as a function of time. Because the isotactic index is usually more or less constant for a catalyst system comprised of $MgCl_2$-supported catalyst and alkoxysilane, this observation is reasonable. Secondly, it is obvious that $w(B)$ increases with time, while $w(C)$ decreases with time. Considering that the PP produced on the type B sites has lower molecular

Table XVI The Characteristics of Each Active Site

	Type A	Type B	Type C
Stereo-regularity	highly isotactic	less isotactic	atactic
Molecular weight	high	medium	low
fraction of PP	fraction A	fraction B	fraction C

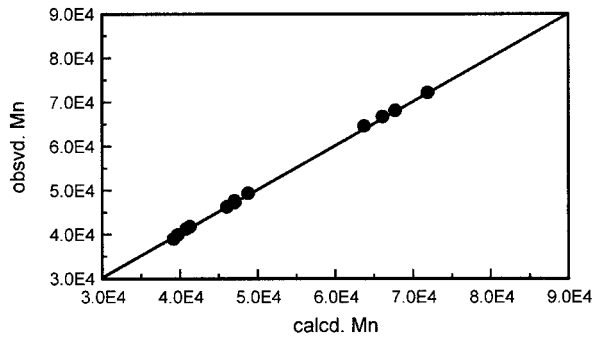

Figure 3 Comparison of the calculated and the observed M_n.

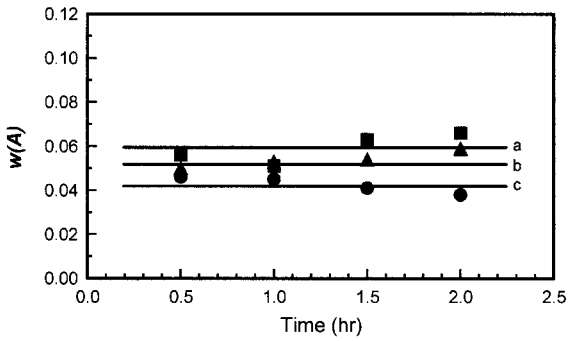

Figure 5 The relationship between time and $w(A)$. (a) $[H_2]$ = 4.7 (vol %), (b) $[H_2]$ = 8.0 (vol %), (c) $[H_2]$ = 11.0 (vol %). This notation is the same in Figure 6 to Figure 13.

weight than that produced on the type C sites, it is natural that molecular weight decreases with time. Therefore, it can be said that the increase in $w(B)$ and decrease in $w(C)$ are at least partially responsible for the observed decrease in molecular weight during polymerization.

Figures 8–13 show the relationship between time and M_n or M_w for each type of active site. These graphs show the change in H_2 response of each active site. Figure 13 shows that $M_w(C)$ slightly decreases with time. In light of the three-site model, this implies that H_2 response of a type C site becomes somewhat more sensitive with time. Interestingly, the H_2 response at the type B site is almost constant. This can be seen in Figures 9 and 12. We can, therefore, say that the change in the H_2 response of a type C site also contributes to the observed decrease in the molecular weight during polymerization.[22]

As a conclusion, it is proposed here that the observed decrease in molecular weight is caused by (a) a decrease in $w(C)$, which is the weight fraction of the polymer with higher molecular weight, and (b) a change in the H_2 response of a type C site.

To better understand the reasons for the narrowing of the MWD, it is necessary to examine the behavior of both M_w and M_n. Figures 9 and 10 show that the M_n of the polymer from the type B and C sites is almost constant, and so is the M_w of that produced on the type B sites, whereas the M_w of that produced on the type C sites decreases with time (Figs. 12 and 13). These results show that the contribution of the component with highest M_w decreases with time. In other words, the quantity of high molecular weight polymer is reduced as a function of time. This is supported by the experimental fact that the weight fractions of the components that are eluted between 123 and 125°C, and between 121 and 123°C decrease with time (see Tables IV–XV). Because M_w is sensitive to the weight fraction of high molecular weight component, this, combined with the fact that the amount of polymer at the lower end of the MWD remains relatively untouched during the reaction, allows us to conclude that the narrowing of MWD is again caused by (a) a decrease in $w(C)$, which is the weight fraction of the polymer with higher

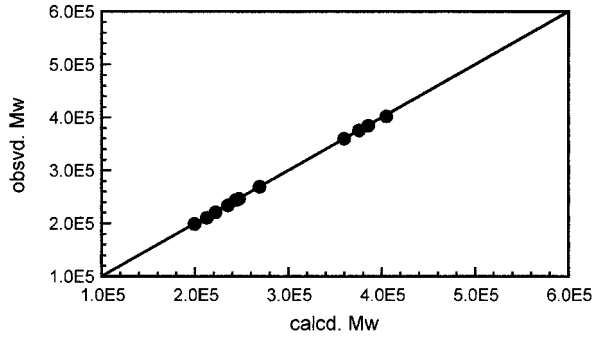

Figure 4 Comparison of the calculated and the observed M_w.

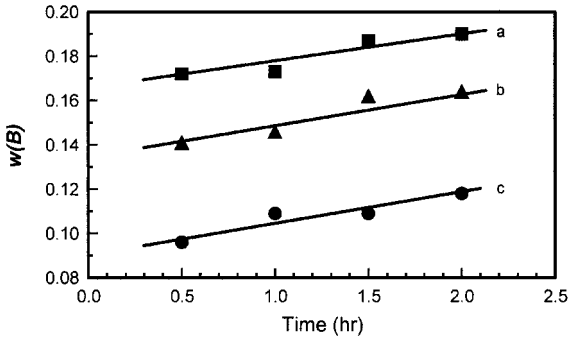

Figure 6 The relationship between time and $w(B)$.

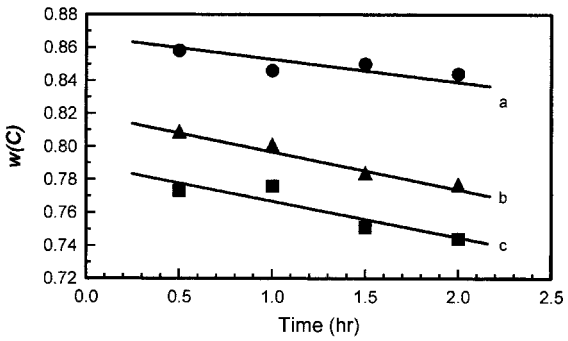

Figure 7 The relationship between time and $w(C)$.

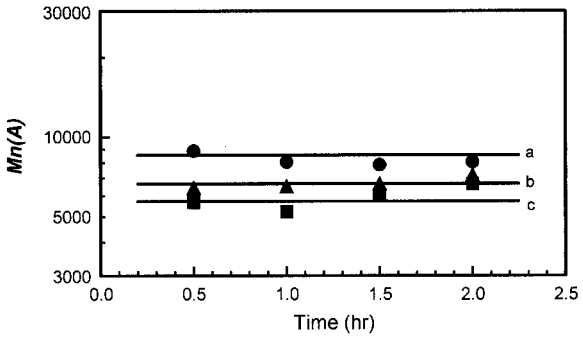

Figure 8 The relationship between time and $M_n(A)$.

molecular weight, and (b) a change in the H_2 response of a type C site.

Deeper Insight Regarding the Mechanism

In the previous section it was demonstrated that the observed decrease in molecular weight and the narrowing of the distribution are both caused by a decrease in $w(C)$ combined with an increase in $w(B)$, and also by a change in the H_2 response at a type C site. This leads us to pose the question: what occurs at the active sites to produce such behavior? Clues as to what happens can be found in the patent literature. For instance, Nakajima et al.[6] showed that molecular weight is almost

Table XVII The Summary of CFC Data Based on Three-Site Model

		Reaction Time (h)			
$[H_2]$ (vol %)	Results	0.5	1.0	1.5	2.0
4.7	$w(A)$	0.046	0.045	0.041	0.038
	$w(B)$	0.096	0.109	0.109	0.118
	$w(C)$	0.858	0.846	0.850	0.844
	$M_n(A)$	8.876E+03	8.057E+03	7.868E+03	8.066E+03
	$M_n(B)$	3.638E+04	3.005E+04	3.179E+04	3.002E+04
	$M_n(C)$	1.467E+05	1.314E+05	1.395E+05	1.297E+05
	$M_w(A)$	2.745E+04	2.556E+04	2.179E+04	1.871E+04
	$M_w(B)$	6.365E+04	5.989E+04	6.327E+04	6.032E+04
	$M_w(C)$	4.636E+05	4.467E+05	4.329E+04	4.168E+05
8.0	$w(A)$	0.050	0.053	0.054	0.059
	$w(B)$	0.141	0.146	0.162	0.164
	$w(C)$	0.809	0.801	0.784	0.777
	$M_n(A)$	6.446E+03	6.529E+03	6.689E+03	7.196E+03
	$M_n(B)$	2.668E+04	2.655E+04	2.802E+04	2.765E+04
	$M_n(C)$	1.078E+05	1.045E+05	1.058E+05	1.021E+05
	$M_w(A)$	1.220E+04	1.294E+04	1.303E+04	1.686E+04
	$M_w(B)$	5.331E+04	5.078E+04	5.350E+04	5.446E+04
	$M_w(C)$	3.226E+05	2.983E+05	2.985E+05	2.899E+05
11.0	$w(A)$	0.056	0.051	0.063	0.066
	$w(B)$	0.172	0.173	0.187	0.190
	$w(C)$	0.773	0.776	0.751	0.744
	$M_n(A)$	5.691E+03	5.230E+03	6.027E+03	6.653E+03
	$M_n(B)$	2.442E+04	2.681E+04	2.576E+04	2.626E+04
	$M_n(C)$	1.001E+05	9.682E+04	9.487E+04	9.252E+04
	$M_w(A)$	1.087E+04	8.845E+03	1.216E+04	1.546E+04
	$M_w(B)$	5.062E+04	5.330E+04	5.075E+04	5.270E+04
	$M_w(C)$	2.752E+05	2.614E+05	2.519E+05	2.532E+05

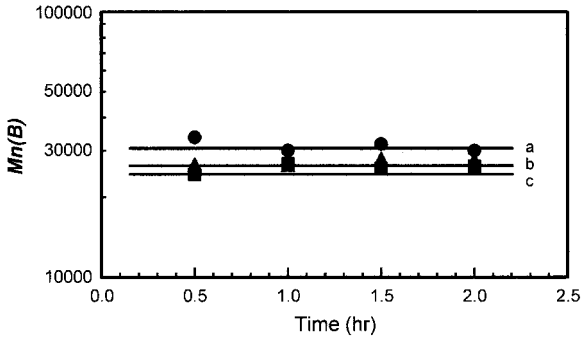

Figure 9 The relationship between time and $M_n(B)$.

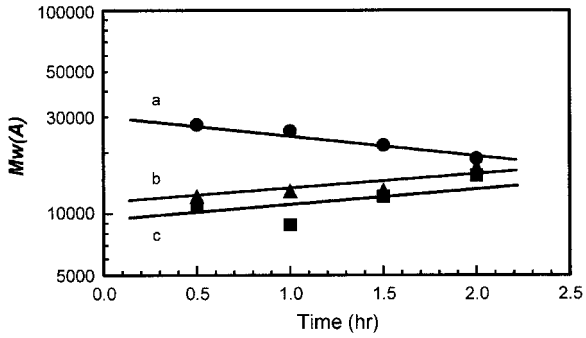

Figure 11 The relationship between time and $M_w(A)$.

constant when a $TiCl_3$ catalyst is used instead of $MgCl_2$-supported catalyst. A big difference between $TiCl_3$ and $MgCl_2$-supported catalyst is the importance of ED, i.e., $TiCl_3$ catalyst can produce relatively highly isotactic PP even without an ED, whereas $MgCl_2$-supported catalyst cannot. With this in mind, it is possible that electron donor might be involved with the implied decrease in $w(C)$, with the increase in $w(B)$, and with the change in the H_2 response at a type C site.

Let us review some well-established concepts related to the nature of alkoxysilane and $MgCl_2$-supported Ziegler-Natta catalyst. In the following, ED represents alkoxysilane as an external donor.

1. Average M_w increases by addition of ED.[23,24] The average M_w also increases with increasing the molar ratio ED/Al, where Al represents alkyl aluminum as the cocatalyst.[1] These facts show that M_w can increase by the interaction of ED and active sites.
2. Two alkoxy groups on a Si atom are necessary for high isotacticity. Only one alkoxy group on a Si atom gives less isotacticity.[23,25]
3. When a Lewis base such as alkoxy silane coordinates to a Mg ion on the (100) surface of a $MgCl_2$ crystal, the equilibrium between mononuclear Ti species (less isospecific site) and binuclear Ti species (isospecific sites) shifts toward the binuclear Ti species.[8,26] Furthermore, an environment that is suitable for isospecific polymerization is formed around the Ti site through the coordination of a Lewis base to a Mg ion neighboring a less isospecific Ti site.[1,27] Thus, the coordination of Lewis base to an Mg ion neighboring a Ti species influences the active site via both a steric and an electronic effect.[1]
4. An alkoxysilane having more than two alkoxy groups reacts with $AlEt_3$. When this reaction occurs, the number of alkoxy groups is reduced. When a monoalkoxysilane is finally formed, it can no longer react with TEA.[1,28]
5. It is supposed that the addition of an elec-

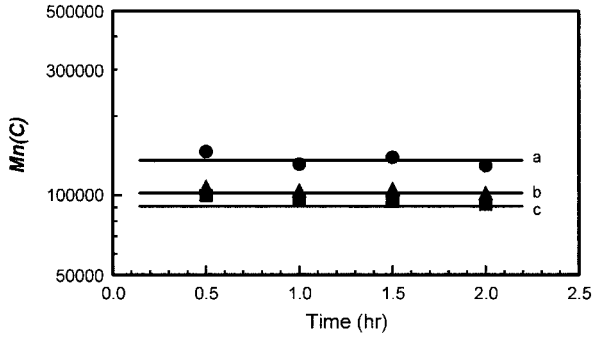

Figure 10 The relationship between time and $M_n(C)$.

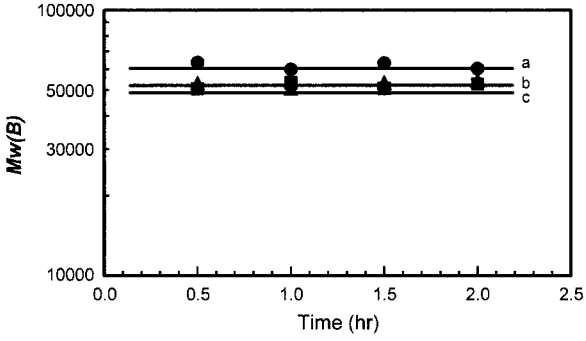

Figure 12 The relationship between time and $M_w(B)$.

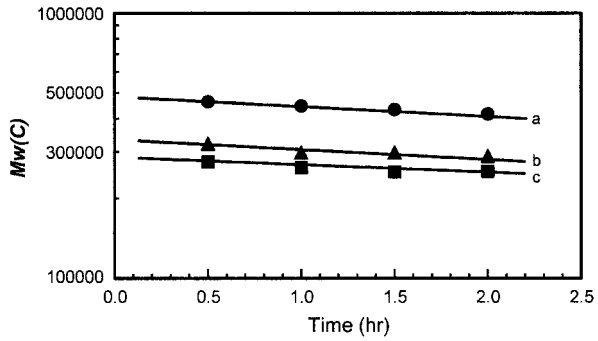

Figure 13 The relationship between time and $M_w(C)$.

tron donor is less effective in reducing the amount of PP rich in syndiotactic sequences.[18] Because syndiotactic sequences are concentrated on so-called atactic PP,[15,16] it implies that the interaction of ED is relatively weak to atactic PP site.

6. By the addition of ED, the isotacticity of the highly isotactic enantiomorphic site is improved.[12,14]
7. The weight fraction of atactic PP is constant when the molar ratio of alkoxysilane and TEA is relatively low.[14,29]
8. Syndiotactic sequences occur as blocks in the same chain[8,15,16] with relatively long isotactic sequences,[8,16] the latter making this material poorly soluble.[15]
9. M_w increases with the elution temperature in TREF and GPC measurement.[18] In other words, M_w increases with increasing isotacticity.
10. The *n*-heptane-soluble polymer fraction is characterized by much lower average molecular weight than the *n*-heptane-insoluble one. From a kinetic point of view, this is mainly due to a lower average rate of chain propagation at such sites compared to that of the isotactic sites.[8,30,31]
11. Part of a less isotactic enantiomorphic site is transformed to a highly isotactic enantiomorphic site. This mechanism is more pronounced with dialkoxysilane.[14] The existence of a less isotactic enantiomorphic site agrees well with the proposal that there is a type of fluctuating site that can randomly form isotactic/syndiotactic stereoblock copolymer.[8,11,14,16,32,33]

Keeping in mind the points mentioned above, we propose the following hypothesis: "An alkoxysilane having the general structure: RR′Si-$(OMe)_2$ is transformed to RR′EtSi(OMe) via the reaction with TEA during polymerization. The proportion of monoalkoxysilane increases with increasing time. This change causes a decrease in the molecular weight, and the narrowing of the polydispersity M_w/M_n because the interaction of monoalkoxysilane weakens, especially at a type C site. Such a weakened interaction of ED results in less isotacticity and a simultaneous decrease in M_w."

Let us explain this hypothesis in more detail. The type A site, which is an aspecific site, produces atactic PP. The interaction between an ED and the type A site is relatively weak (cf. 5). For this reason, the stereo-regularity of polymer produced on the type A site does not change, regardless of the transformation of the ED during polymerization (cf. 4). In addition, the type A site continues to produce PP with low molecular weight because of its low chain propagation rate (cf. 10). As a result, the type A site produces atactic PP with low molecular weight for the entire reaction. Also $w(A)$, which is the weight fraction of atactic PP, is almost constant because the ratio of ED/TEA was very low in this study (cf. 8).

On the other hand, the type C site, which is a highly isotactic enantiomorphic site, produces highly isotactic PP, and is influenced by the ED (cf. 3). Because of the interaction between the ED and the type C site, the isotacticity of the polymer produced on these type C sites increases (cf. 6). This interaction is strongest at the beginning of polymerization because ED is rich in dialkoxysilane at this point (cf. 2 and 11). With increasing time, the proportion of monoalkoxysilane increases (cf. 4), which in turn, leads to a decrease in the isotacticity of the polymer formed at a type C site (cf. 2). Simultaneously, a fraction of the type C sites that was formed from type B sites through the latter's interaction with the dialkoxysilane reverts to its original form, i.e. type B sites (cf. 2 and 11). As a result, $w(C)$ decreases with time and $w(B)$ increases simultaneously. Because $M_w(B)$ is lower than $M_w(C)$, this is one of the causes of decrease in molecular weight with time. Moreover, because less isotactic PP has lower M_w (cf. 1, 9, and 10), the average M_w produced from a type C site decreases with time. This also contributes to the observed decrease in molecular weight with time.

The type B site, which is a less isotactic enantiomorphic site, produces less isotactic PP. Because a type B site is originally a fluctuating one,

part of the type B sites is transformed to a type C site when it interacts with an ED, which is rich in dialkoxysilane at the beginning of polymerization (cf. 11). The rest of the type B sites produces less isotactic PP, even in the presence of ED. Note that a type B site where less isotactic PP is produced has a weaker interaction with the ED (cf. 5). The less isotactic PP is a kind of stereoblock PP consisting of relatively long isotactic sequences and relatively short syndiotactic sequences (cf. 8). Due to the existence of the relatively long isotactic sequences, such a stereoblock PP is less soluble to solvent compared to atactic PP (cf. 8). In addition, because of its lower isotacticity, the solubility of such stereoblock PP is higher than highly isotactic PP. This is why we observe such PP in the elution temperature range between 95 and 111°C. In the course of polymerization, the proportion of monoalkoxysilane increases with time (cf. 4). As mentioned above, it causes a decrease in $w(C)$ and an increase in $w(B)$. Meanwhile the stereoregularity and the H_2 response in most of the type B sites remains more or less constant, even when the proportion of monoalkoxysilane increases, because the interaction of the ED with most of the type B sites is relatively weak (cf. 5). Thus, most of the type B sites continue to produce PP with an almost constant isotacticity and M_w.

To summarize, $w(A)$ is almost constant, $w(B)$ increases with time, while $w(C)$ decreases with time, and $M_w(A)$ and $M_w(B)$ do not change significantly, while $M_w(C)$ decreases. On the other hand, the average M_n does not noticeably change during these transformations because M_n is a much stronger function of the lower molecular tail of the MWD. In addition, the effect of the ED is weak at the active sites where PP with low molecular weight is produced, which means that variations in the concentration and the nature of ED do not have a strong influence on M_n. These factors all contribute to the narrowing of the M_w/M_n as the reaction progresses. A schematic diagram of the events that probably take place during polymerization is presented in Figure 14.

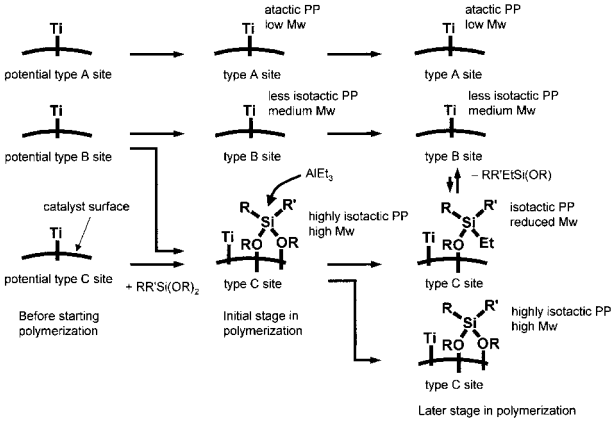

Figure 14 A probable scheme for the time dependency of molecular weight.

CONCLUSION

It is demonstrated that the molecular weight of PP decreases, and that its molecular weight distribution becomes narrower as a function of time in the liquid pool polymerization of propylene on $MgCl_2$-supported Ziegler-Natta catalyst combined with a dialkoxysilane ED. A CFC study showed that this phenomenon occurs due to the decrease in the fraction of the active sites that produce PP with high molecular weight and high isotacticity. Based on the well-established concepts and our experimental facts, a mechanism that explains these observations has been proposed.

REFERENCES

1. Albizatti, E.; Gianinni, U.; Collina, G.; Noristi, L.; Resconi, L. Polypropylene Handbook; Moore, E. G., Ed.; Carl Hanser Verlag: Munich, 1996.
2. Prasetya, A.; Liu, L.; Lister, J.; Watanabe, F.; Mitsutani, K.; Ko, G. H. Chem Eng Sci 1999, 54, 3263.
3. Tanaka, E.; Mitsutani, K.; Watanabe, F.; Yukawa, K.; Shimizu, F.; Natori, Y. DECHEMA Monographs, 6th International Workshop on Polymer Reaction Engineering, Berlin, 1998, p. 135.
4. Samson, J. J. C.; Weickert, G.; Heerze, A. E.; Westerterp, K. R. A I Ch E J 1998, 44, 1424.
5. Samson, J. J. C.; Bosman, P. J.; Weickert, G.; Westerterp, K. R. J Polym Sci Part A Polym Chem Ed 1999, 37, 219.
6. Nakajima, M.; Nakano, A.; Furuhashi, H.; Ueki, S. Jpn Pat. 11-140114 (1999), Tonen Chemical Co.
7. Spitz, R.; Bobichon, C.; Guyot, A. Makromol Chem 1989, 190, 707.
8. Corradini, P.; Busico, V.; Cipullo, R. Catalyst Design for the Tailor-Made Polyolefins, Proceedings of the International Symposium on Catalyst Design for the Tailor-made Polyolefins, Kanazawa, March 10–12, 1994, p. 21.
9. Kakugo, M.; Miyatake, T.; Naito, Y.; Mizunuma, K. Macromolecules 1998, 21, 314.
10. Kakugo, M.; Miyatake, T.; Mizunuma, K.; Kawai, Y. Macromolecules 1988, 21, 2309.

11. Kakugo, M. Catalyst Design for the Tailor-Made Polyolefins, Proceedings of the International Symposium on Catalyst Design for the Tailor-made Polyolefins, Kanazawa, March 10–12, 1994, p. 129.
12. Cheng, H. N. J Appl Polym Sci 1988, 35, 1639.
13. Strictly speaking, Kakugo has proposed that stereoblock PP (SB) and syndio-specific PP (SP) can be also formed. In this article, these PPs, if any, were included in IP_2 or AP because their isotacticity was lower than IP_1.
14. Härkönen, M.; Seppälä, J. V.; Salminen, H. Polym J 1995, 27, 256.
15. Paukkeri, R.; Väänänen, T.; Lehtinen, A. Polymer 1993, 34, 2488.
16. Busico, V.; Corradini, P.; De Biasio, R.; Landriani, L.; Segre, A. L. Macromolecules 1994, 27, 4521.
17. Busico, V.; Cipullo, R.; Monaco, G.; Talarico, G.; Vacatello, M.; Chadwick, J. C.; Segre, A. L.; Sudmeijer, O. Macromolecules 1999, 32, 4173.
18. Kioka, M.; Makio, H.; Mizuno, A.; Kashiwa, N. Polymer 1994, 35, 580.
19. Kawamura, H.; Hayashi, T.; Inoue, Y.; Chujo, R. Macromolecules 1989, 22, 2181.
20. The fraction A, B, and C are not necessarily completely identical with AP, IP_2, and IP_1 that Kakugo et al.[9,10,11] proposed. However, they are similar to AP, IP_2, and IP_1, especially insofar as the molecular weight and isotacticity increase in this order.
21. We classified the PP samples into three fractions A, B, and C. Therefore, "real polymer" here means the original PP sample, which consists of the fractions A, B, and C.
22. The behavior of the type A site is complicated. However, it does not matter because $w(A)$ is small enough compared with $w(B)$ and $w(C)$.
23. Seppälä, J. V.; Härkönen, M. Makromol Chem 1989, 190, 2535.
24. Chadwick, J. C.; Miedema, A.; Sudmeijer, O. Macromol Chem Phys 1994, 195, 167.
25. Spitz, R.; Bobichon, C.; LlauroDarricades, M. F.; Guyot, A.; Duranel, L. J Mol Catal 1989, 56, 156.
26. Busico, V.; Corradini, P.; DeMartino, L.; Proto, A.; Savino, V.; Albizzati, E. Makromol Chem 1985, 186, 1279.
27. Ishii, K.; Mori, T.; Fujita, T. Kobunshi Ronbunshu 1994, 51, 685.
28. Vähäsarja, E.; Pakkanen, T. T.; Pakkanen, T. A.; Iiskola, E.; Sormunen, P. J Polym Sci Part A Polym Chem 1987, 25, 3241.
29. As a factor that influences stereo-regularity, the authors think that the concentration of external donor is much better than the molar ratio of external donor and cocatalyst. But here, we cited the original expression described in the Härkönen's report.
30. Keii, T.; Terano, M.; Kimura, K.; Ishii, K. Transition Metals and Organometallics as Catalysts for Olefin Polymerization; Kaminsky, W.; Sinn, H., Ed.; Springer Verlag: Heidelberg, 1987, p. 3.
31. Terano, M.; Kataoka, T.; Keii, T. J Polym Sci Part A Polym Chem Ed 1990, 28, 2035.
32. Härkönen, M.; Seppälä, J. V.; Chûjô, R.; Kogure, Y. Polymer 1995, 36, 1499.
33. Paukkeri, R.; Iiskola, E.; Lehtinen, A.; Salminen, H. Polymer 1994, 35, 2636.